Journal of Applied Data Sciences
Vol. 7, No. 3, September 2026, pp. 2265-2275

ISSN 2723-6471
2265

ACO-Optimized DSTATCOM for Reactive Power Compensation in PV-Integrated Weak Grids

Rajasree R[1,*], Lakshmi D[2], Stalin K[3], Karthick Manoj R[4], P Jeyarani[5]

[1,2,5]Department of EEE, AMET University, Chennai, India

[3]Department of Marine, AMET University, Chennai, India

[4]Centre for Data Science and Sustainable Technologies, INTI International University, Nilai, N. Sembilan, Malaysia

(Received: February 15, 2026; Revised: April 20, 2026; Accepted: July 18, 2026; Available online: August 9, 2026)

Abstract

The integration of photovoltaic generation into weak distribution grids introduces voltage instability, reactive power imbalance, harmonic distortion, and prolonged transient response due to low short-circuit capacity and high grid impedance. This study proposes an Ant Colony Optimization-based Distribution Static Synchronous Compensator for improving voltage regulation and power quality in a PV-integrated weak grid. The optimization algorithm is used to tune the proportional–integral controller parameters by minimizing a composite objective involving PCC voltage deviation, reactive power error, total harmonic distortion, feeder power loss, and settling time. The proposed system is modeled in MATLAB/Simulink and evaluated against two benchmark configurations: an uncompensated weak-grid system and a conventional PI-controlled DSTATCOM. The results show that the proposed controller reduces PCC voltage deviation from 0.060 pu to 0.012 pu and reactive power demand from 150 kVAR to 5 kVAR. Total harmonic distortion decreases from 6.5% to 1.6%, while the power factor improves from 0.78 lagging to 0.995. In addition, feeder real-power losses are reduced from 45 kW to 28 kW, and the settling time decreases from 1.8 s to 0.5 s. These findings demonstrate that ACO-based controller tuning provides consistent improvements in voltage regulation, reactive power compensation, harmonic mitigation, feeder efficiency, and dynamic recovery under weak-grid operating conditions.

Keywords: Ant Colony Optimization, DSTATCOM, Photovoltaic System, Reactive Power Compensation, Weak Grid, Voltage Regulation, Total Harmonic Distortion, Process Innovation

1. Introduction

The increasing penetration of photovoltaic (PV) generation in distribution networks has introduced significant challenges related to voltage regulation, reactive power balance, harmonic distortion, and overall grid stability. These issues become more critical in weak grids, which are characterized by low short-circuit capacity, high grid impedance, and limited capability to accommodate rapid variations in power injection. Under such conditions, fluctuations in solar irradiance, load demand, and inverter operating points can produce considerable voltage deviations and deteriorate power quality at the point of common coupling (PCC). Previous studies have shown that coordinated voltage and reactive power control is essential for maintaining reliable operation under varying source and load conditions [1], [2].

Weak-grid conditions also degrade the synchronization and control performance of converter-interfaced renewable energy systems. The interaction between high grid impedance and inverter control loops, phase-locked loops (PLLs), and resonance characteristics may lead to oscillatory responses or even instability. To address these challenges, various advanced control strategies have been proposed, including grid-impedance compensation, adaptive predictive control, virtual synchronous generator (VSG) control, and dual active compensation [3]–[6]. Although these approaches improve converter stability and dynamic performance, their implementation often requires accurate system models, additional control layers, or complex parameter coordination, particularly under dynamically changing grid and loading conditions. Flexible AC Transmission System (FACTS) devices provide an effective alternative for improving voltage stability and power quality through dynamic reactive power compensation. Among distribution-level FACTS devices,

*Corresponding author: Rajasree R (raji.sree1988@gmail.com)
DOI: https://doi.org/10.47738/jads.v7i3.1467

the Distribution Static Synchronous Compensator (DSTATCOM) has attracted considerable attention because of its fast response, bidirectional reactive power capability, and effectiveness in mitigating voltage fluctuations and nonlinear-load effects. Previous studies have demonstrated that DSTATCOM can significantly improve voltage regulation and power quality in weak-grid renewable energy systems and distribution networks containing nonlinear loads [1], [7]. In addition, other converter-based compensation technologies, such as Unified Power Quality Conditioners (UPQCs) and hybrid STATCOM configurations, have been investigated to further enhance voltage compensation, reduce switching losses, and improve fault ride-through capability [8], [9].

Despite these advantages, the overall performance of a DSTATCOM strongly depends on the proper tuning of its control parameters. Conventional proportional–integral (PI) controllers are typically designed for a limited operating range and may exhibit excessive overshoot, longer settling times, or reduced compensation accuracy when grid strength, PV generation, and load characteristics vary. Consequently, optimization-based controller tuning has received increasing attention in recent years. Genetic algorithm (GA)-based optimization has been successfully applied to enhance reactive power management and synchronization in grid-connected PV systems [10], while hybrid population-based optimization techniques have been investigated for optimal reactive power dispatch under complex operating conditions [11]. These findings indicate that metaheuristic optimization offers an effective approach for determining controller parameters in nonlinear and multi-objective power system applications.

Nevertheless, most existing studies investigate inverter synchronization, reactive power dispatch, or DSTATCOM controller optimization as separate problems. Comprehensive evaluations that simultaneously consider voltage deviation, reactive power compensation, total harmonic distortion (THD), feeder real-power losses, power factor, and transient settling time within the same PV-integrated weak-grid framework remain limited. Furthermore, the benefits of optimization should be assessed not only against an uncompensated system but also against a conventionally controlled DSTATCOM to determine whether the additional optimization stage consistently improves system performance under varying operating conditions.

Accordingly, this study proposes an Ant Colony Optimization (ACO)-based DSTATCOM control framework for reactive power management in a PV-integrated weak grid. The ACO algorithm is employed to optimize the controller parameters by minimizing voltage deviation, reactive power error, harmonic distortion, and transient response time. The proposed method is implemented in MATLAB/Simulink and evaluated under varying PV generation and load conditions. Its performance is compared with two benchmark configurations: (i) a system without a FACTS device and (ii) a DSTATCOM employing a conventional PI controller. The comparative evaluation focuses on PCC voltage deviation, reactive power compensation, total harmonic distortion, power factor, feeder real-power losses, and settling time to provide a comprehensive assessment of the proposed optimization-based control strategy.

2. Literature Review

The integration of converter interfaced renewable energy resources into weak electrical networks has intensified research on voltage regulation, reactive power control, and power quality enhancement. Weak grids are particularly vulnerable to renewable energy intermittency because their low short circuit capacity and high equivalent impedance amplify voltage fluctuations and reduce the stability margin of converter interfaced systems. Previous studies have demonstrated that DSTATCOM based compensation effectively improves voltage regulation and reactive power support in weak grid connected renewable energy systems [12], while hybrid voltage and reactive power control strategies have been proposed to maintain stable operation under uncertain source and load conditions [13]. These findings indicate that adaptive compensation methods are essential when system operating conditions cannot be accurately represented by fixed control parameters.

The stability of converter interfaced systems under weak grid conditions has also received considerable attention. Various control strategies have been proposed to mitigate the adverse effects of grid impedance on converter synchronization and dynamic performance. These include grid impedance compensation techniques [14], adaptive predictive control for resonance suppression [15], virtual synchronous generator (VSG) control to improve synchronization characteristics [16], and dual active compensation for voltage source converters operating under very weak grid conditions [17]. Although these methods significantly improve converter level stability and synchronization performance, they primarily focus on the internal dynamics of power electronic converters rather than providing comprehensive distribution level compensation that simultaneously addresses voltage deviation, reactive power demand, harmonic distortion, and feeder losses.

Converter based Flexible AC Transmission System (FACTS) devices have therefore become an effective solution for enhancing distribution network performance. Among these technologies, Unified Power Quality Conditioners (UPQCs) have demonstrated effective voltage compensation capability in microgrid applications [18], while DSTATCOM has proven effective in mitigating voltage fluctuations and compensating nonlinear load effects [19]. In addition, hybrid STATCOM configurations have been developed to improve converter efficiency, reduce switching losses, and enhance fault ride through capability [20]. Overall, these studies confirm that voltage source converter based compensators provide rapid reactive current injection, harmonic mitigation, and improved voltage profiles. Nevertheless, their overall performance remains highly dependent on controller parameter tuning, and conventional proportional integral (PI) controllers may experience performance degradation under varying PV generation, load demand, and grid strength conditions.

To overcome the limitations of conventional controller tuning, metaheuristic optimization techniques have been increasingly adopted in renewable energy control applications. Evolutionary optimization methods have been successfully applied to improve reactive power management and synchronization in grid connected PV systems [21]. These studies demonstrate that optimization algorithms can effectively determine controller parameters for nonlinear and multi objective power system problems. Among various optimization approaches, Ant Colony Optimization (ACO) offers an attractive balance between global exploration and local exploitation, making it suitable for DSTATCOM controller tuning under dynamically changing operating conditions.

Despite these advances, existing studies generally investigate converter synchronization, reactive power dispatch, or DSTATCOM controller optimization as separate research topics. Comprehensive assessments that simultaneously evaluate uncompensated systems, conventional PI controlled DSTATCOM, and optimization based DSTATCOM using multiple performance indicators, including voltage deviation, reactive power compensation, total harmonic distortion (THD), power factor, feeder real power losses, and transient settling time, remain limited. This research gap provides the primary motivation for the integrated evaluation presented in this study.

3. Methodology

3.1. System Configuration and Simulation Design

The proposed system consists of a photovoltaic generation unit, a voltage-source inverter, a weak distribution grid, a nonlinear load, and a shunt-connected Distribution Static Synchronous Compensator (DSTATCOM). The weak-grid condition is represented by a short-circuit ratio of 2.5 and a feeder impedance of $0.05 + j0.30$ pu. The DSTATCOM is installed at the point of common coupling (PCC) to regulate the bus voltage, compensate reactive power demand, improve the power factor, and reduce current harmonics. This configuration follows the use of converter-based compensation for voltage and power-quality enhancement in weak grids [1], [3], [7].

The proposed PV integrated weak grid system is modeled and simulated in MATLAB/Simulink. The simulation parameters are summarized in table 1, which presents the electrical characteristics of the PV generation system, distribution network, DSTATCOM, and simulation environment. The PV array is rated at 500 kW and operates with a nominal DC voltage of 600 V, while the grid connected inverter is rated at 550 kVA to ensure sufficient conversion capacity during variations in PV output. The weak grid condition is represented by a short circuit ratio (SCR) of 2.5 and a grid impedance of $(0.05 + j0.30)$pu, reflecting a network with limited voltage support and relatively high sensitivity to power injection [22]. The DSTATCOM is rated at 200 kVA and employs a 700 V DC link with a $2000\ \mu$Fcapacitor to provide fast reactive power compensation and maintain stable DC link operation. The simulation is conducted over a period of 5 s, during which changes in PV generation and load demand are introduced to evaluate both the transient and steady state performance of the proposed control strategy under realistic operating conditions.

Table 1. Simulation and system parameters

Parameter	Symbol	Value
Rated PV power	$(P_{\mathrm{PV,r}})$	500 kW
PV array nominal voltage	(V_{PV})	600 V DC
PV inverter rating	(S_{inv})	550 kVA
Grid voltage	(V_g)	1.0 pu
Grid frequency	(f_g)	50 Hz
Short-circuit ratio	SCR	2.5
Grid/line impedance	(Z_g)	(0.05+j0.30) pu
DSTATCOM rated capacity	(S_{DSTATCOM})	200 kVA
DC-link reference voltage	(V_{dc}^*)	700 V
DC-link capacitance	(C_{dc})	(2000~\mu\text{F})
Simulation duration	(T_s)	5 s

The short-circuit ratio is expressed as:

$$SCR = \frac{S_{\mathrm{sc}}}{S_{\mathrm{inv}}} \tag{1}$$

S_{sc} is the short-circuit capacity of the grid at the PCC and S_{inv} is the rated apparent power of the PV inverter. A lower SCR indicates a weaker grid and stronger interaction between the inverter controller and the grid impedance [5], [8]. The reactive power exchanged at the PCC is calculated from the three-phase voltage and current components as:

$$Q_{\mathrm{PCC}} = \frac{3}{2}\left(v_q i_d - v_d i_q\right) \tag{2}$$

v_d and v_q denote the PCC voltage components, and i_d and i_q denote the corresponding current components in the synchronous reference frame. Under voltage-oriented control, the d-axis is aligned with the PCC voltage, resulting in $v_q \approx 0$. Consequently, the reactive power can be controlled predominantly through the quadrature-axis current i_q.

Figure 1 illustrates the overall architecture of the proposed PV integrated weak grid system incorporating an Ant Colony Optimization (ACO) based DSTATCOM controller. The main power path consists of a PV array connected to a grid connected inverter, which injects active power into the point of common coupling (PCC). The PCC is connected to a weak utility grid through the grid impedance $\boldsymbol{Z_g}$, while a nonlinear load is connected in parallel to represent practical distribution network conditions that introduce reactive power demand and harmonic distortion.

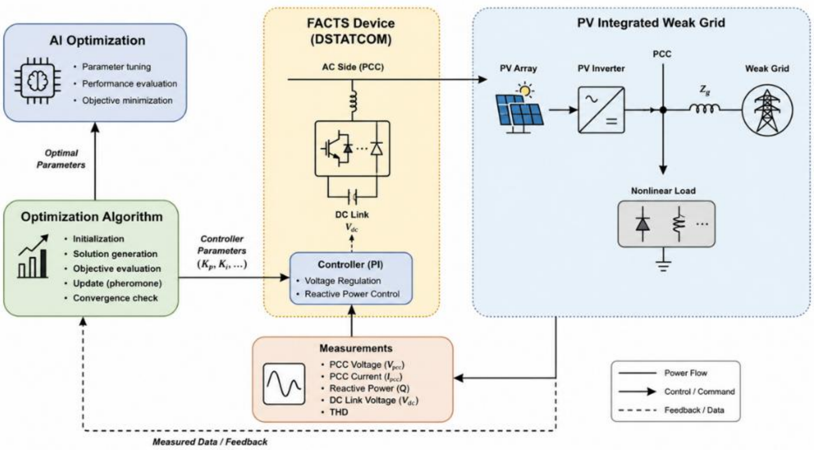

Figure 1. Proposed PV-integrated weak-grid system with ACO-optimized DSTATCOM

ISSN 2723-6471

A DSTATCOM is installed in shunt at the PCC to provide dynamic reactive power compensation and voltage support. The compensator consists of a voltage source converter supplied by a DC link capacitor and regulated by a conventional PI controller. During system operation, the DSTATCOM injects or absorbs reactive current according to the PCC operating conditions, thereby improving voltage regulation, reducing reactive power demand, and mitigating power quality disturbances caused by renewable power fluctuations and nonlinear loads. The controller continuously receives measurements from the PCC, including the PCC voltage (V_{PCC}), reactive power (Q), DC link voltage (V_{dc}), and total harmonic distortion (THD). These measured variables are used to evaluate the system operating condition and provide the feedback required for DSTATCOM control.

Unlike an online adaptive controller, the ACO algorithm operates as an offline parameter optimization stage. Based on the measured system characteristics and predefined objective function, the optimization algorithm determines the optimal PI controller parameters before the simulation or system operation begins. The optimized controller gains are then applied to the DSTATCOM controller, while the controller itself performs real time voltage regulation and reactive power compensation during operation. This architecture separates the computationally intensive optimization process from the real time control loop, enabling improved dynamic performance without increasing the online computational burden.

3.2. DSTATCOM Control and ACO-Based Parameter Optimization

The DSTATCOM controller regulates the PCC voltage and DC-link voltage through two control loops. The outer control loop generates the reference reactive-current component based on the PCC voltage error, while the DC-link controller maintains the energy balance of the converter. The corresponding voltage errors are defined as:

$$e_v(t) = V_{\mathrm{PCC}}^* - V_{\mathrm{PCC}}(t) \tag{3}$$

and:

$$e_{\mathrm{dc}}(t) = V_{\mathrm{dc}}^* - V_{\mathrm{dc}}(t) \tag{4}$$

V_{PCC}^* and V_{dc}^* represent the PCC and DC-link reference voltages, respectively. The conventional PI control signal is formulated as:

$$u(t) = K_p e(t) + K_{i \int_0^t e(\tau)} d \tag{5}$$

K_p and K_i are the proportional and integral gains. In the proposed method, these gains are not selected manually. Instead, Ant Colony Optimization is used to identify the gain combination that produces the minimum voltage error, reactive power error, harmonic distortion, and transient settling time. Optimization-based parameter selection is appropriate because weak-grid behavior is nonlinear and varies with PV output, grid impedance, and load operating conditions [4], [11]. Each ant represents one candidate controller parameter vector,

$$\theta_m = \left[K_{p,v}, K_{i,v}, K_{p,\mathrm{dc}}, K_{i,\mathrm{dc}}\right]_m \tag{6}$$

m denotes the candidate solution. The fitness of each candidate is evaluated using the following composite objective function:

$$J(\theta) = w_1 \int_0^T |e_v(t)| dt + w_2 \int_0^T |e_Q(t)| dt + w_{3\mathrm{THD_I}} + w_4 t_s + w_5 P_{\mathrm{loss}} \tag{7}$$

Note:

$$e_Q(t) = Q_{\mathrm{PCC}}^* - Q_{\mathrm{PCC}}(t) \tag{8}$$

Here, $\mathrm{THD_I}$ is the current total harmonic distortion, t_s is the settling time, P_{loss} is the feeder real-power loss, and $w_1 - w_5$ are weighting coefficients. Before optimization, each objective component should be normalized to prevent quantities with larger numerical scales from dominating the fitness function:

$$\widetilde{x_k} = \frac{x_k - x_k^{min}}{x_k^{max} - x_k^{min}} \tag{9}$$

ability that ant mmm selects candidate region j is determined by:

$$p_{mj} = \frac{[\tau_j]^{\alpha}[\eta_j]^{\beta}}{\sum_{l\in\Omega_m}[\tau_l]^{\alpha}[\eta_l]^{\beta}} \tag{10}$$

τ_j is the pheromone intensity, η_j is the heuristic desirability, α controls the influence of pheromone information, β controls the influence of heuristic information, and Ω_m is the feasible candidate set. Following the evaluation of all candidate solutions, the pheromone value is updated as:

$$\tau_j^{(r+1)} = (1-\rho)\tau_j^{(r)} + \sum_{m=1}^{M} \Delta\tau_{mj}^{(r)} \tag{11}$$

4. Results and Discussion

4.1. Voltage Regulation and Reactive Power Compensation

The performance of the proposed ACO optimized DSTATCOM was evaluated by comparing three operating configurations: (i) the uncompensated weak grid system, (ii) a DSTATCOM employing a conventional PI controller, and (iii) the proposed DSTATCOM with ACO optimized controller parameters. All simulation scenarios were performed using identical PV generation, grid impedance, load conditions, and disturbance profiles to ensure that the observed performance differences were solely attributable to the compensation strategy and controller tuning.

Figure 2 compares the PCC voltage waveforms obtained from the three evaluated configurations. All cases maintain a sinusoidal voltage waveform with the nominal amplitude under steady state conditions. However, the uncompensated system exhibits the largest deviation from the reference voltage when operating under weak grid conditions, whereas the inclusion of a DSTATCOM improves voltage regulation by providing dynamic reactive power support. The proposed ACO optimized DSTATCOM produces the waveform that most closely follows the reference voltage, indicating improved voltage regulation and enhanced dynamic compensation capability. The close overlap of the three waveforms during steady state operation indicates that the primary benefit of the proposed controller is achieved during transient operating conditions, where optimized controller parameters enable faster voltage recovery and reduced voltage deviation compared with the conventional PI controller. The quantitative comparison of voltage regulation performance is presented in the subsequent analysis, where the maximum voltage deviation, transient response, and other power quality indices are evaluated for all three configurations.

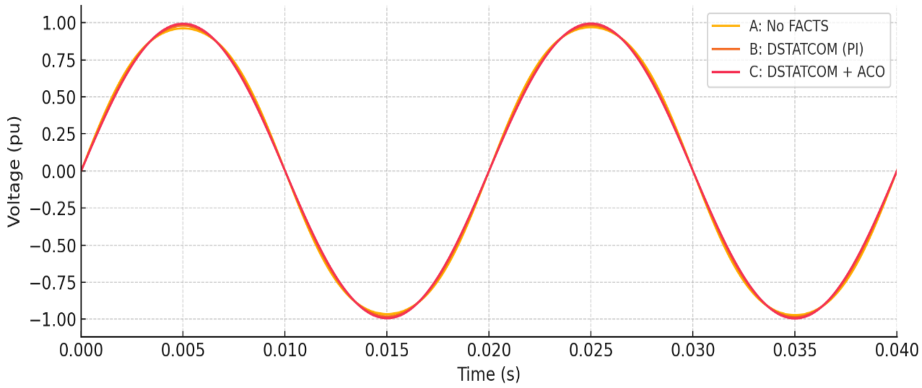

Figure 2. PCC voltage response for the three evaluated configurations

This improvement indicates that the optimized controller generates a more accurate compensating-current reference when the PCC voltage changes. The conventional PI controller provides substantial voltage support, but its fixed gains produce a larger residual deviation than the optimized configuration. The result is consistent with previous studies reporting that DSTATCOM-based compensation improves weak-grid voltage regulation, while optimized gain selection can enhance transient and steady-state control performance [1], [7]. The voltage deviation results can be summarized as:

$$\Delta V_{\text{reduction}} = \frac{0.06 - 0.012}{0.06} \times 100 = 80\% \tag{12}$$

The corresponding reactive power response is presented in figure 3.

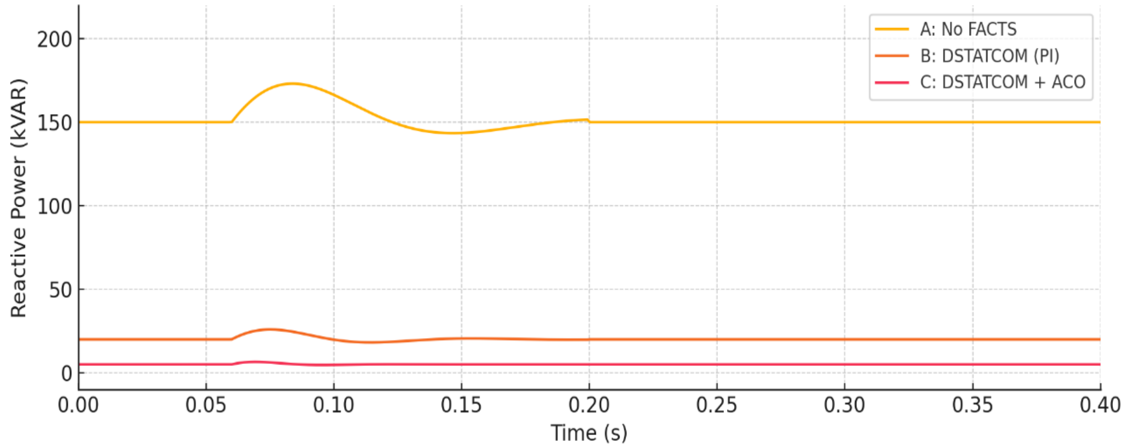

Figure 3. Reactive power at the PCC under uncompensated, PI-controlled, and ACO-optimized operation

Without compensation, the reactive power demand at the PCC reaches approximately 150 kVAR. The conventional DSTATCOM reduces this value to 20 kVAR, while the ACO-optimized DSTATCOM limits the residual reactive power to approximately 5 kVAR. The proposed configuration therefore achieves a reactive power reduction of:

$$\eta_Q = \frac{150 - 5}{150} \times 100 = 96.7\% \quad (13)$$

The lower residual reactive power indicates that the proposed controller more effectively balances the reactive component demanded by the load and the weak grid. It also reduces the reactive burden on the upstream feeder. This reduction contributes directly to the improvement in power factor and feeder efficiency discussed in the following subsection.

4.2. Harmonic Distortion, Power Factor, and Power Losses

The harmonic performance of the three evaluated configurations is compared in figure 4, which presents the total harmonic distortion (THD) measured at the PCC under identical operating conditions. Figure 4 shows that the uncompensated system exhibits the highest THD value of 6.5%, indicating significant waveform distortion caused by the combined effects of inverter switching, nonlinear loads, and the high impedance of the weak grid. The installation of a conventional PI controlled DSTATCOM reduces the THD to 3.2% by injecting compensating currents that suppress harmonic components and improve the quality of the PCC voltage waveform.

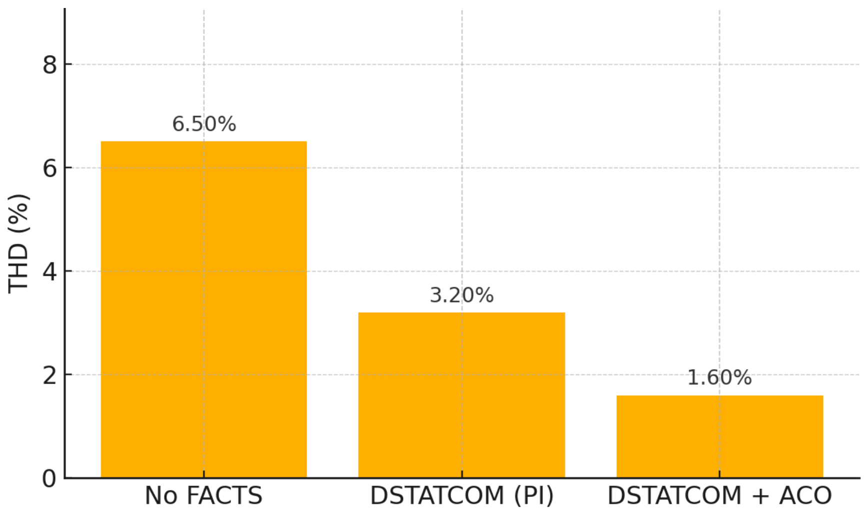

Figure 4. THD comparison for the three evaluated configurations

The proposed ACO optimized DSTATCOM achieves the lowest THD of 1.6%, representing a reduction of approximately 75.4% compared with the uncompensated system and 50% compared with the conventional PI controlled DSTATCOM. The improved harmonic performance is attributed to the optimized controller parameters, which enable more accurate reactive current regulation and faster dynamic compensation under varying operating conditions. These results demonstrate that the ACO based tuning strategy not only enhances voltage regulation but also significantly improves power quality by reducing harmonic distortion to a level well below the 5% limit recommended by IEEE Std. 519. The relative reduction obtained by the proposed controller is:

$$\text{THD Deduction} = \frac{6.5 - 1.6}{6.5} \times 100 = 75.4\% \tag{14}$$

The reported 1.6% THD indicates a substantial improvement in current waveform quality. The difference between the conventional and optimized controllers suggests that controller tuning affects not only voltage regulation but also the accuracy of harmonic-current compensation. Nevertheless, the paper should explicitly state whether the THD value was obtained using the MATLAB Powergui FFT analysis tool, a discrete Fourier transform, or Equation (14). The measurement window and number of harmonic orders should also be reported to ensure reproducibility. The power-factor response is presented in figure 5.

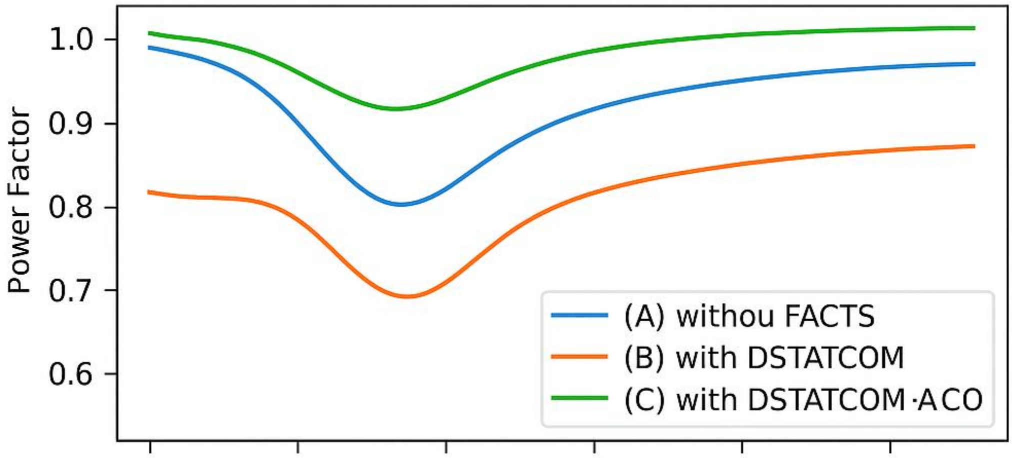

Figure 5. Power-factor response under the three control configurations

In the absence of compensation, the system operates at a lagging power factor of 0.78. The conventional DSTATCOM improves the power factor to 0.97 lagging, while the proposed ACO-optimized DSTATCOM achieves a near-unity power factor of 0.995. The improvement is produced by reducing the phase displacement between the PCC voltage and current through controlled reactive current injection. The increase in power factor from 0.78 to 0.995 is equivalent to:

$$\text{PF Increase} = \frac{0.995 - 0.78}{0.78} \times 100 = 27.6\% \tag{15}$$

Although this percentage expresses the numerical increase, the more meaningful interpretation is that the proposed controller moves the operating point close to unity power factor. Consequently, the apparent power required to deliver the same amount of active power is reduced. The feeder real-power loss decreases from 45 kW in the uncompensated configuration to 33 kW with the conventional DSTATCOM and 28 kW with the proposed controller. The reduction achieved by the optimized configuration is:

$$\text{Loss Deduction} = \frac{45 - 28}{45} \times 100 = 37.8\% \tag{16}$$

This reduction can be attributed to the lower reactive current flowing through the feeder. Since line losses are proportional to the square of the RMS current, improved reactive power compensation and power factor reduce the current magnitude required for power transfer.

4.3. Dynamic Response and Overall Performance Comparison

The settling time provides an indication of how rapidly each configuration recovers after a disturbance. The uncompensated system requires approximately 1.8 s to reach steady operation. The conventional PI-controlled DSTATCOM reduces this period to 0.9 s, whereas the ACO-optimized controller achieves a settling time of approximately 0.5 s. The corresponding improvement is:

$$\text{Settling Time Deduction} = \frac{1.8 - 0.5}{1.8} \times 100 = 72.2\% \quad (18)$$

The shorter settling time indicates that the optimized controller reaches the required compensating-current level more rapidly and with a lower residual error. This result is important in PV-integrated weak grids because irradiance and load changes can occur repeatedly, leaving limited time for the controller to recover before the next operating disturbance. The overall quantitative comparison is presented in table 2.

Table 2. Performance comparison of the evaluated control configurations

Performance metric	Without FACTS device	DSTATCOM with conventional PI	ACO-optimized DSTATCOM	Improvement over uncompensated system
PCC voltage deviation	0.060 pu	0.025 pu	0.012 pu	80.0%
Reactive power at PCC	150 kVAR	20 kVAR	5 kVAR	96.7%
Total harmonic distortion	6.5%	3.2%	1.6%	75.4%
Power factor	0.78 lagging	0.97 lagging	995	27.6% numerical increase
Feeder real-power losses	45 kW	33 kW	28 kW	37.8%
Settling time	1.8 s	0.9 s	0.5 s	72.2%

The results demonstrate a consistent performance hierarchy across all evaluated metrics. The uncompensated configuration produces the largest voltage deviation, reactive power demand, harmonic distortion, feeder loss, and settling time. Introducing the conventional DSTATCOM substantially improves the system, confirming that dynamic reactive power compensation is effective for PV-integrated weak-grid operation. However, the ACO-optimized configuration produces the best result for every reported metric.

The benefit of the proposed approach is therefore not limited to a single control objective. ACO-based parameter tuning simultaneously improves voltage regulation, reactive power compensation, harmonic mitigation, power factor, feeder efficiency, and transient recovery. Compared with optimization methods previously applied to renewable-energy control and reactive power dispatch [4], [11], the present implementation focuses specifically on tuning the DSTATCOM controller under a PV-integrated weak-grid configuration.

Nevertheless, the results should be interpreted within the scope of the simulation. The manuscript currently reports one set of aggregated performance values and does not provide repeated runs, sensitivity analysis, or statistical variability. Since ACO is a stochastic optimization algorithm, the final paper should ideally report the mean, standard deviation, best value, and worst value obtained over multiple independent optimizations runs.

5. Conclusion

This study developed an ACO-optimized DSTATCOM control framework for reactive power management and power-quality enhancement in a PV-integrated weak grid. Ant Colony Optimization was used to tune the PI controller parameters based on multiple operational objectives, including PCC voltage deviation, reactive power demand, harmonic distortion, feeder losses, and transient settling time. The proposed configuration was evaluated against an uncompensated system and a conventional PI-controlled DSTATCOM under the same simulation conditions.

The results show that the ACO-optimized DSTATCOM consistently outperformed both benchmark configurations. PCC voltage deviation was reduced from 0.060 pu to 0.012 pu, while reactive power demand decreased from 150 kVAR to 5 kVAR. The proposed controller also reduced total harmonic distortion from 6.5% to 1.6%, improved the power factor from 0.78 lagging to 0.995, decreased feeder real-power losses from 45 kW to 28 kW, and shortened the settling time from 1.8 s to 0.5 s. These results indicate that optimization-based parameter tuning improves not only steady-state voltage and reactive power regulation but also harmonic mitigation, feeder efficiency, and transient recovery.

The findings confirm that a properly tuned DSTATCOM can provide effective dynamic support for renewable-energy systems connected to weak distribution networks. However, the conclusions remain limited to the modeled simulation scenarios and parameter settings. Future work should validate the proposed controller using hardware-in-the-loop or laboratory experiments, examine its robustness under a wider range of short-circuit ratios and disturbance conditions, and evaluate the statistical consistency of ACO across multiple independent optimizations runs. Comparative testing against other optimization algorithms would also help determine whether the observed improvements are specific to ACO or reflect the broader benefit of metaheuristic controller tuning.

6. Declarations

6.1. Author Contributions

Conceptualization: R.R., L.D., S.K., K.M.R., and P.J.; Methodology: L.D.; Software: R.R.; Validation: R.R., L.D., S.K., K.M.R., and P.J.; Formal Analysis: R.R., L.D., S.K., K.M.R., and P.J.; Investigation: R.R.; Resources: L.D.; Data Curation: L.D.; Writing—Original Draft Preparation: R.R., L.D., S.K., K.M.R., and P.J.; Writing—Review and Editing: L.D., R.R., S.K., K.M.R., and P.J.; Visualization: R.R.; All authors have read and agreed to the published version of the manuscript.

6.2. Data Availability Statement

The data presented in this study are available on request from the corresponding author.

6.3. Funding

The authors received no financial support for the research, authorship, and/or publication of this article.

6.4. Institutional Review Board Statement

Not applicable.

6.5. Informed Consent Statement

Not applicable.

6.6. Declaration of Competing Interest

The authors declare that they have no known competing financial interests or personal relationships that could have appeared to influence the work reported in this paper.

References

[1] A. F. Zobaa, "Mixed-integer distributed ant colony multi-objective optimization of single-tuned passive harmonic filter parameters," *IEEE Access*, vol. 7, no. Mar., pp. 44862–44870, Mar. 2019, doi: 10.1109/ACCESS.2019.2903910.

[2] H. Mohamad, N. A. F. Roslan, K. Naidu, N. A. Salim, and Z. M. Yasin, "Optimal placement of electric vehicles charging station using ant colony optimization," *IEEE Int. Conf. Power Eng. Appl.*, vol. 2025, no. Mar., pp. 19–24, Mar. 2025, doi: 10.1109/ICPEA65539.2025.11198221.

[3] Y. Dhieb, M. Yaich, M. Bouzguenda, and M. Ghariani, "MPPT optimization using ant colony algorithm: Solar PV applications," *IEEE Int. Conf. Sci. Technol. Autom. Control Comput. Eng.*, vol. 2022, no. Dec., pp. 503–507, Dec. 2022, doi: 10.1109/STA56120.2022.10019072.

[4] L. Xue, J. Jun, and W. Jian, "Research on fault location of low voltage distribution network based on improved ant colony algorithm," *Int. Forum Electr. Eng. Autom.*, vol. 2020, no. Nov., pp. 759–762, Nov. 2020, doi: 10.1109/IFEEA51475.2020.00161.

[5] R. Kumar, R. Singh, and H. Ashfaq, "Stability enhancement of multi-machine power systems using ant colony optimization-based static synchronous compensator," *Comput. Electr. Eng.*, vol. 83, no. 1, pp. 1–12, May 2020, doi: 10.1016/j.compeleceng.2020.106589.

[6] L. Lin, C. Zhang, X. Li, and Y. Zhang, "Load adjustment planning method for distribution network transformer areas based on simulated annealing-quantum ant colony algorithm," *Int. Conf. Electron. Circuits Inf. Eng.*, vol. 2025, no. Apr., pp. 854–858, Apr. 2025, doi: 10.1109/ECIE65947.2025.11087063.

[7] B. H. Al-Majali, A. F. Zobaa, I. Pisica, and O. Ceylan, "Optimal STATCOM allocation using mixed integer distributed ant colony optimization," *IEEE Conf. Power Electron. Renewable Energy*, vol. 2023, no. Nov., pp. 1–6, Nov. 2023, doi: 10.1109/CPERE56564.2023.10119602.

[8] A. A. Ogunsina, M. O. Petinrin, O. O. Petinrin, E. N. Offornedo, J. O. Petinrin, and G. O. Asaolu, "Optimal distributed generation location and sizing for loss minimization and voltage profile optimization using ant colony algorithm," *SN Appl. Sci.*, vol. 3, no. 2, pp. 1–12, Feb. 2021, doi: 10.1007/s42452-021-04226-y.

[9] W. Miao, X. Zhao, C. Wang, S. Chen, P. Gao, and Q. Li, "A GNN-enhanced ant colony optimization for security strategy orchestration," *Symmetry*, vol. 16, no. 9, pp. 1–15, Sep. 2024, doi: 10.3390/sym16091183.

[10] O. M. Kamel, A. A. Z. Diab, T. D. Do, and M. A. Mossa, "A novel hybrid ant colony-particle swarm optimization techniques based tuning STATCOM for grid code compliance," *IEEE Access*, vol. 8, no. Mar., pp. 41566–41587, Mar. 2020, doi: 10.1109/ACCESS.2020.2976828.

[11] N. Bhoopal, D. S. M. Rao, B. K. Narukullapati, I. Kasireddy, and D. G. Kumar, "Selective harmonic elimination based THD minimization of a symmetric 9-level inverter using ant colony optimization," *Math. Model. Eng. Probl.*, vol. 8, no. 5, pp. 769–774, Oct. 2021, doi: 10.18280/mmep.080512.

[12] N. H. Abdul Kahar, Y. Yahya, I. Ahmad, I. Alhamrouni, and B. Ismail, "Multi-objectives optimization in feasibility enhanced extended ant colony algorithm for design of undamped passive filter," *Int. Conf. Eng. Technol. Technopreneurship*, vol. 2023, no. Sep., pp. 118–123, Sep. 2023, doi: 10.1109/ICE2T58637.2023.10540526.

[13] P. Goli, S. Makkena, S. R. Gampa, and D. Das, "Fuzzy ant colony optimization technique for predefined performance of distribution systems considering DGs and shunt capacitors," *North Amer. Power Symp.*, vol. 2019, no. Oct., pp. 1–6, Oct. 2019, doi: 10.1109/NAPS46351.2019.9000250.

[14] X. Li and Z. Yin, "Research on communication networking method in low voltage distribution station area based on improved ant colony algorithm," *Int. Conf. Electron. Mater. Inf. Eng.*, vol. 2022, no. Jul., pp. 856–860, Jul. 2022.

[15] Y. Zhang *et al.*, "Research on optimization of power line carrier communication routing algorithm for low-voltage distribution network," *Int. Trans. Electr. Energy Syst.*, vol. 31, no. 11, pp. 1–12, Nov. 2021, doi: 10.1002/2050-7038.12656.

[16] C. Qian and A. Wang, "Distribution network reconfiguration based on improved differential evolution ant colony algorithm," *Int. Conf. Big Data, Artif. Intell. Internet Things Eng.*, vol. 2022, no. Aug., pp. 234–240, Aug. 2022, doi: 10.1109/ICBAIE56435.2022.9985818.

[17] A. Q. Abdulrasool and L. T. Al-Bahrani, "Multi-objective constrained optimal power flow based on enhanced ant colony system algorithm," *Int. Symp. Adv. Topics Electr. Eng.*, vol. 2021, no. May, pp. 1–6, May 2021, doi: 10.1109/ATEE52255.2021.9425082.

[18] N. W. Budiantari, R. N. Hasanah, and H. Suyono, "Design of wind turbine battery charging control a buck-boost converter with PID control optimized by ant colony optimization," *Electr. Power, Electron., Commun., Controls Inform. Seminar*, vol. 2024, no. Jul., pp. 44–49, Jul. 2024, doi: 10.1109/EECCIS62037.2024.10840117.

[19] N. Dagade Godha, R. Dagade, V. Bapat, and I. Korachagaon, "Polydomous ant colony optimization for distributed generation and capacitors placement in the context of techno-economic and environmental objectives," *Iran. J. Sci. Technol., Trans. Electr. Eng.*, vol. 49, no. 4, pp. 2125–2143, Dec. 2025, doi: 10.1007/s40998-025-00882-7.

[20] L. Zeng, "Power line communication networking method for low voltage distribution network based on ant colony algorithm," *Lecture Notes Data Eng. Commun. Technol.*, vol. 2022, no. Mar., pp. 782–787, Mar. 2022, doi: 10.1007/978-3-030-89508-2_101.

[21] X. Xu, M. Wu, and H. Yang, "Research on substation grounding grid design based on improved ant colony algorithm," *Int. Symp. Semiconductor Electron. Technol.*, vol. 2025, no. Aug., pp. 762–765, Aug. 2025, doi: 10.1109/ISSET66828.2025.11184981.

[22] S. Dhivya and S. Prakash, "Power quality assessment in grid-connected solar PV systems using deep learning techniques," *J. Appl. Data Sci.*, vol. 6, no. 2, pp. 1192–1208, Jun. 2025, doi: 10.47738/jads.v6i2.655.